A Thesis Presented to

The Faculty of Alfred University

EFFECTS OF POST-TREATMENT ABRASION ON DYNAMIC FATIGUE OF CHEMICALLY STRENGTHENED GLASS

by

Nicholas Tostanoski

In Partial Fulfillment of
the Requirements for
The Alfred University Honors Program

05/07/2018

Under the Supervision of:

Chair: Dr. William LaCourse

Committee Members:

Dr. Steven Pilgrim

Dr. Garrett McGowan

ACKNOWLEDGEMENTS

I would like to thank my parents Michele and Tim Tostanoski, my brother Alexander, and my family for always supporting me, looking out for me, providing me with guidance and advice, and most importantly their never-ending love. I would like to thank Dr. William LaCourse for mentoring throughout this thesis and for teaching me in class over the past two years. I would also like to thank my advisor Dr. Steven Pilgrim, who has been supporting me through the Materials Science and Engineering program since freshman year. I would like to thank my friends, Dan, David, and Jenna, I gained over the past four years while attending Alfred University.

Table of Contents

LIST OF TABLES

LIST OF FIGURES

ABSTRACT

Effects of post-ion exchange abrasion on strength and fatigue of soda-lime silicate glass rods, were determined using four-point bend tests. Dynamic fatigue tests were carried out by varying the strain rate over 2 orders of magnitude in air or after a short immersion in water. Ion exchange was carried out at 450^{o}C for 4 or 16-hours. Following the ion exchange treatment, the glass rods were abraded using sand particles between 212 to 149µm and 106 to 63µm. The resulting strength (MOR) values were plotted using Weibull statistics. Dynamic fatigue plots showing the effect of stressing rate on strengths were also plotted, and the slow crack growth constant (n) was determined for each combination of ion exchange time and post-abrasion. Results indicate that the surface stresses induced by chemical strengthening reduces effects of stress-induced slow crack growth. However, anomalous, and unexpected large reductions in fatigue behavior requires that additional measurements, be carried out before any interpretations can be provided.

INTRODUCTION

In glass science and engineering glass is often ion exchanged (IOX). This ion exchanging is a process of chemically strengthening a glass through diffusion of ions within the glass with an external ion source. “Ions from the glass diffuse out of the sample, while ions from the source diffuse into the sample”.[1] Sodium ions diffuse out while the potassium ions, from a molten KNO_3 bath, are diffusing into the glass. It is the difference in size of these ions which allow for a chemically strengthening. Figure 1 contains an image of the glass surface after an IOX procedure has been completed.

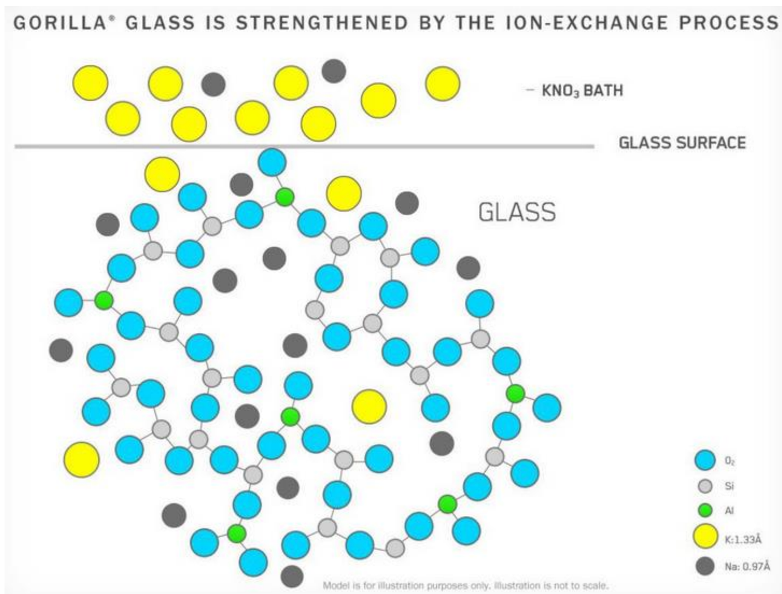

Figure 1: Ion-exchanged glass surface[2]

Glass is brittle material whose fracture behavior is dependent upon the surface flaws present. The strength at failure for glass depends if any treatments have been applied to the glass. The failure of glass is not determined by the bonding of the structure. Glasses fracture strengths are never able to reach their theoretical strengths due to surface flaws present on the glass. These surface flaws are detrimental to the possibility of a glass reaching its theoretical strength. The theoretical strength of a glass can be described by the following equation 1, in which E is the Young’s or Elastic Modulus. As stated before, the theoretical strength will not be reached due to flaws located on the surface of the glass. “These flaws act as stress concentrations, increasing the local stresses to levels exceeding the theoretical strength and causing fracture of the glass”.[1]

Equation 1: $\sigma theo = \frac{E}{5}$

Griffith was able to account for the surface flaws and derived an expression to determine the glass failure, which is located in equation 2. This shows σ_f is the failure stress, γ surface energy, and c* is the critical crack length of the crack growth. In order for a crack to grow it must reach the critical crack length.[1]

Equation 2: $\sigma f = \sqrt{\frac{2E\gamma}{\pi c*}}$

There is variation in the glass fracture strengths due to the surface flaws. The crack tip propagation is dependent upon having a crack of suitable length and a stress great enough to grow the crack. The experimental method used to test the failure strength affects the value obtains. Three-point bend tests will receive a different failure strength than four-point bend tests. This is due to the area being tested during the failure strength test. The stress applied to the rods during the testing is maximum at different locations for the two tests. For "a 3-point bend test occurs at the point directly opposite the load point, while the maximum stress in a 4-point bend test occurs over the region between the two load points".[1] The three-point bend tests have more variation in failure strengths due to the maximum stress at one point, when compared to the variation in the four-point bend test. "The probability of a critical flaw for a given stress occurring within the region of maximum stress is greater".[1]

Due to the inability of determining an exact MOR for brittle solids failure statistics are used. Weibull distributions are used to describe the glass fracture strengths. The Weibull modulus has physical significance to the glass samples being tested and it is the distribution of the samples strengths. If the Weibull modulus is very large (infinite) then all the samples are breaking at one stress and is predictable. If the Weibull modulus is very small or low, then the samples are breaking at multiple stresses and is unpredictable. In general, it is best to have a large Weibull modulus because it shows that your sample is consistent and all break at the same stress/strength.

Static fatigue is when a constant load is placed on a glass sample until failure. The glass strength decreased with time, due to the atmosphere or moisture, interacting with the crack tip, which results in crack growth while the constant load is applied. A higher failure strength is obtained when the load is increased at a fast rate. Meanwhile, when the load is increased at a slow rate the failure strength is lower. When the load rate is continually increased at a constant rate until failure, the glass is experiencing dynamic fatigue. Glass fatigue is due to the interaction of the glass surface flaw with water, which is also called stress-enhanced corrosion. This interaction can be described by equation 3. This shows the glass network displayed by the Si-O-Si bonds, which has oxygen acting as a bridging oxygen, and interacts with the water to form Si-OH. This Si-OH has the oxygen acting as a nonbridging oxygen and reduces the connectivity of the glass structure, specifically at the tip. This process can be found in Figure 2. The result of this interaction between the crack tip surface and water is a sharpening of the crack tip. This stress-enhanced corrosion of glass is influenced by the humidity, if there is a higher humidity then there is more water present and the reaction will likely drive to the right side in the creation of non-bridging oxygens. If the crack tip is under tension, then they are more prone to the chemical attack from the water. If there is a slower loading rate during strength testing, or static fatigue testing, then this reaction will have time to proceed and result in sharpening of the crack tip. Meanwhile, if the loading rate is faster the reaction will not have time to proceed and there will be no stress-enhanced corrosion occurring.[1]

Glass strengths are decreased through moisture and susceptible to static fatigue. In static fatigue, there is a constant load being applied to the sample for an extended period of time. During this process the glasses are susceptible to subcritical crack growth. "This leads to failure over time at loads which might be safe when considering instantaneous loading".[3]

Equation 3: $Si - O - Si + H_2O = 2\ Si - OH$

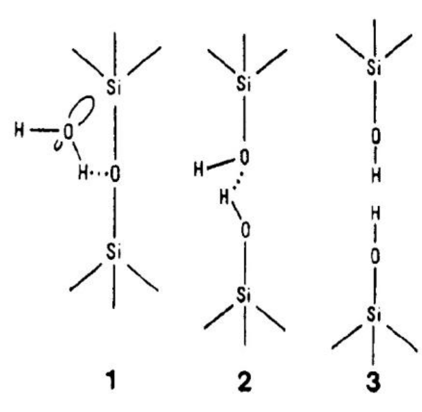

Figure 2: Stress-enhanced corrosion breaks the bonds at the crack tip, crack sharpening[1]

Glass and other brittle materials experience fracture through the rapid crack propagation. Fracture mechanics accounts for the relationships between numerous factors such as material properties, crack-producing flaws, stress levels, and crack propagation mechanisms. The fracture strength of brittle solids is much lower when compared to the theoretical strengths. This is due to the flaws or cracks present at the surface and interior of the solid. These flaws can be so crucial because an applied stress will be concentrated at the crack tip. The localized stress around the crack decreases as the distance from the crack increases. The Inglis equation, which is located in equation 4, approximates the maximum stress at the crack tip. Where σ_{tip} is the stress at the crack tip, σ_{ap} is the applied stress, σ_o is the applied tensile stress, r is the radius of curvature for the crack, and c is the length of the surface crack or half the length of the interior crack. The ratio of σ_{tip}/σ_{ap} is also termed the stress concentration factor K_{1C}, also called the critical stress intensity factor. This stress intensity factor "is simply a measure of the degree to which an external stress is amplified at the tip of a crack".[4] The stress intensity factor can be described by equation 5.

Equation 4: $\sigma tip = 2\sigma ap \left(\frac{c}{r}\right)^2$

Equation 5: $K1C = \frac{\sigma tip}{\sigma ap} = 2\left(\frac{c}{r}\right)^{1/2}$

Dynamic fatigue has a sample continuously increasing stress at a constant rate until fracture. The slow crack growth constant or stress enhanced corrosion constant, n value, can be determined from a dynamic fatigue plot. A typical dynamic fatigue curve can be found below in Figure 3. The n value is affected by composition, environment, and state of stress. The slope of the curve would be m = 1/(n+1). Sub-critical crack growth is when the crack is not a critical length for a fast fracture. However, the crack slowly grows until it reaches the crucial length required for failure. The environment and the crack velocity are in line with one another in for the slow crack growth region. Water is getting into the crack tip and slowly breaking the bonds and lengthening the crack. The slow crack growth constant shows how susceptible the glass is to slow crack growth or water assisted failure. The slow crack (sub-critical) crack growth equation can be found in Equation 6.

Equation 6: $V = AK^n$

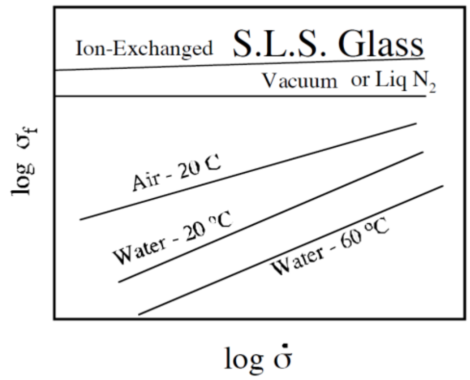

Figure 3: Typical dynamic fatigue curve

Glass fatigue is due to the interaction between glass and water, water reduces the connectivity of the glass and grows the crack. The n value represents how susceptible the glass is to water assisted failure. Strength decreases with time, due to moisture (humidity) or atmosphere interacting with the crack tip, the result is crack growth. If there is no water present, no chemical attack at the crack tip occurs. If the crack tip is in tension, then the crack is more prone to chemical attack. Soda-lime-silicate glasses typically have n values from 10 to 15.[6]

EXPERIMENTAL PROCEDURE

The AR glass rods have a diameter of 4 mm and were cut to a length of three inches. The glass rods were tested in two mediums; air and water, and both will be discussed below in detail. The glass rods were ion-exchanged (IOX), abraded, and strength tested, in this order. The air medium had two IOX times, two sand particle size abrasions, and three testing rates. The water medium had one IOX time, one abrasion level, and three rates. In both medium cases strength testing for as received (nothing done to the glass), ion-exchange, and abrasion without ion-exchange was performed.

The ion-exchange (IOX) was performed in an Lindberg/Blue M Crucible Furnace, for either 4 or 16-hours at 450^{o}C. The samples were loaded into a stainless steel sample holder, which can fit 100 samples, and were placed into a bath of KNO_3. The IOX bath's temperature varies by ± 10^{o}C, which, for present tests did not cause significant differences in treatments. The air medium had both the 4 and 16-hour ion-exchange bath times, while the water medium just had the 16-hour bath time.

Sand was used as the abrasive material. It was sieved using an auto tap W.S. Tyler Incorporated machine. The particle sizes collected from the sieve are as follows, in A.S.T.M. specification numbers; 30, 40, 70, 100, 120, 140, 230, and 325. In micrometer (μm) mesh size; 595, 425, 212, 149, 125, 106, 63, and 45 μm. The two particle sizes which were chosen to abrade the glass rods which were tested in the air medium are +149 and +63. The glass rods tested in the water had a particle size of +149μm. In which the + represents what sand particles which passed through the first mesh and were retained in the second mesh. The +149 sand particles have a range of 212 to +149μm, while the +63 sand particles have a range of 106 to +63μm. 400 grams of the specific sand particle size was placed inside of a jar mill. Ten samples were placed inside of the container at a time and were abraded (ABR) for fifteen minutes at a speed of 40% on a U.S. Stoneware Mill.

The glass rods were tested using a four-point bend test on a Instron. The support span length was 40 mm, while the load span length was 20 mm, giving the four-point bend test a span ratio of 2. The testing room is a climate-controlled environment, in which the relative humidity varies from 5% to 30%, depending on the weather for the specific day testing took place. The glass rod samples tested in air were tested at three different rates; 1, 7, and 20 mm/min.

Meanwhile the water strength tested rods had rates of 0.2, 2, and 20 mm/min. For the “water medium” samples, rods were submerged in water for a time of one to three minutes prior to the strength test, followed by fracture in air. The data for each test was recorded and the maximum flexure load was obtained, in order to determine the modulus of rupture (MOR), or σ_f.

To assure that the test procedure used above to determine water environment effects was valid, an additional test in which the glass was four-point bend tested in water was performed (Break in Water). These samples were abraded at +149μm, and abrasion before an IOX in combination, and were tested at a rate of 2 mm/min.

DATA

Following the completing of the four-point bend tests, which determine the maximum flexural load, the modulus of rupture (MOR), or the stress at failure (σ_f), can be calculated. The MOR can be determined by equation 7. In which P is the maximum flexure load [N], D is the diameter [D], L is the support length span [mm], a is the load length span [mm], and the MOR is in units of MPa. The maximum flexure load and MOR for both testing mediums, along with the average and standard deviation for MOR can be found in the Appendix.

Equation 7: $MOR = \frac{8P(L-a)}{\pi D^3}$

A Weibull "probability of failure" plot was created for each specific testing condition including the rate at which the samples were tested. Weibull plots can be created using the MOR value and F, where F is the "probability of failure at a particular stress" and equals the "number of samples failing at a specific stress minus 0.5 divided by the total number of samples". (Equation 8). The y-axis of a Weibull modulus contains F, specifically ln(ln(1/(1-F))), and the x-axis contains the ln(MOR). Once the Weibull plot has been created if a linear trendline for the data is created (e.g. the slope of the data) for each specific group and testing rate. The slope is the Weibull modulus, "m", and is a measure of the scatter in the data. All Weibull moduli can be found in Table 1.

The n value, or stress enhanced carrion or slow crack growth constant, can be determined by taking the average MOR for each testing rate for a specific group and plotting it. The y-axis is log(σf) and the x-axis is log(σrate). Following the creation of the plot a trendline is added, in which using the slope of the line (m) (Equation 9) one can determine the n value by following equation 10.

Equation 8: $F = \frac{(\# \, failing \; at \; \sigma - 0.5)}{N}$

Equation 9: $slope \; (m) = \frac{1}{(n+1)}$

Equation 10: $n = \frac{1}{m} - 1$

The Weibull plot for all samples tested in air and which were as just received (AR), ion exchanged (IOX), or just abrasion(ABR) at the different stress rates can be found in Figure 4.

This figure allows for each comparison of Weibull modulus and the failing strength for each different type of sample. Figure 5 contains the Weibull plot for the samples which had the combination of ion exchanging followed by abrasion for all testing rates. Finally, the water Weibull plot for the samples which were submerged in water for one to two minutes before testing can be found in Figure 6.

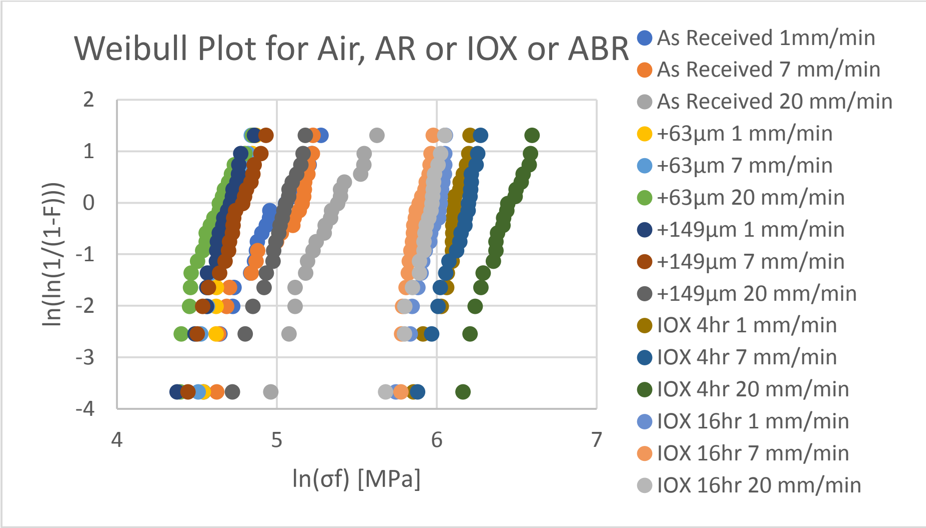

Figure 4: Weibull Plot for air testing of samples with either as received, just abrasion, or just ion exchange

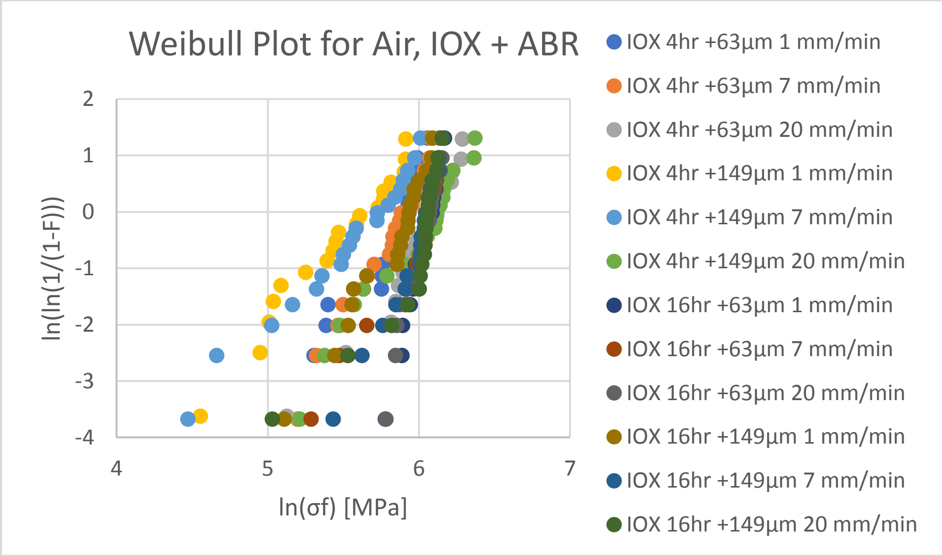

Figure 5: Weibull plot for air testing of samples with the combination of ion exchanging followed by abrasion

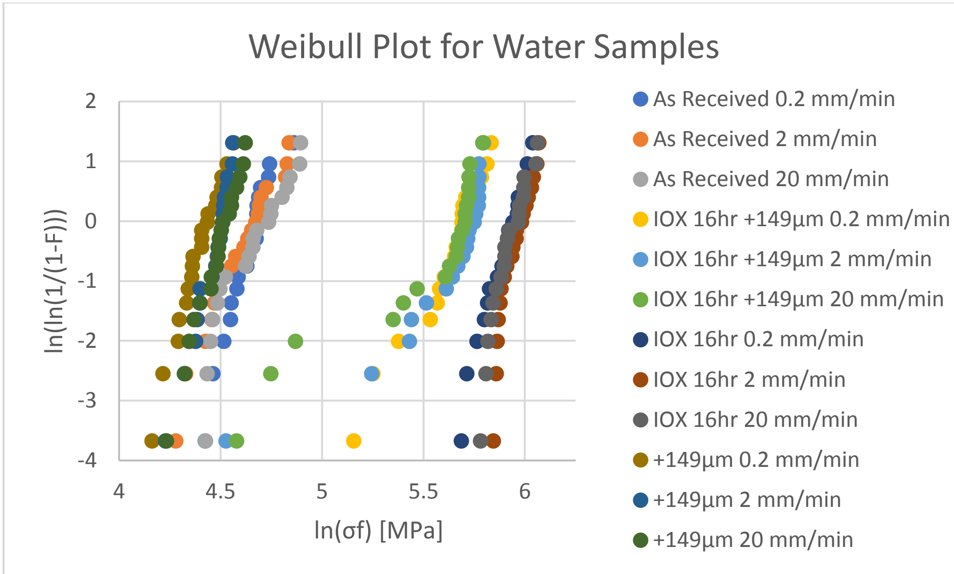

Figure 6: Weibull plot for the water samples as received, just ion exchange or abrasion and then the combination

The dynamic fatigue plots for the as received, just IOX, or just ABR can be found in Figure 7. This figure, when the axes are both on a LOG scale can be used to calculate the n value. Figure 8 contains the dynamic fatigue plot for the samples which were IOX and ABR tested. Meanwhile the samples which were submerged in water before breaking have their dynamic fatigue plot in Figure 9.

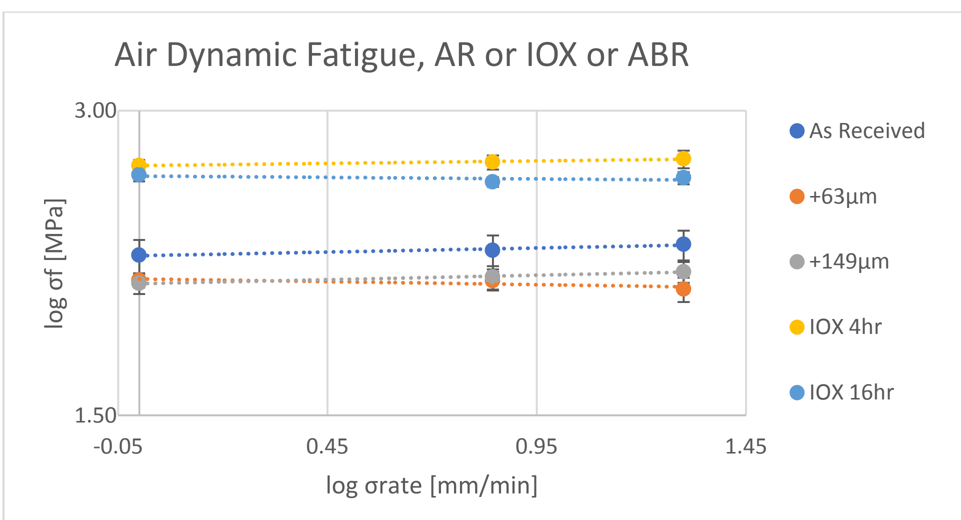

Figure 7: Dynamic fatigue plot for the water testing of as received, just abrasion or just ion exchange

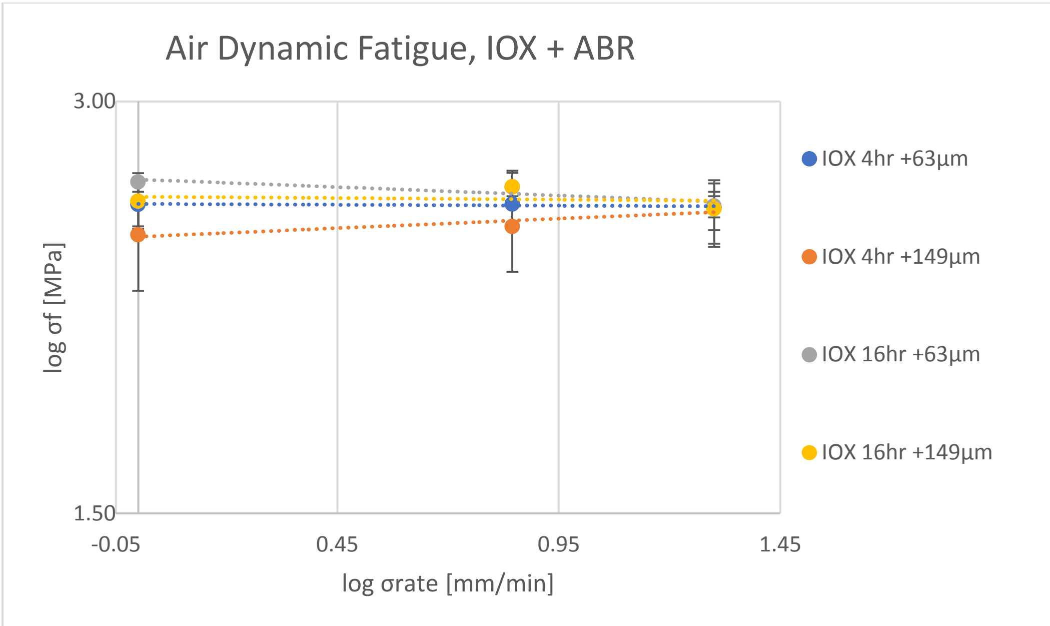

Figure 8: Dynamic fatigue plot for air testing of samples which were abraded and then ion exchanged

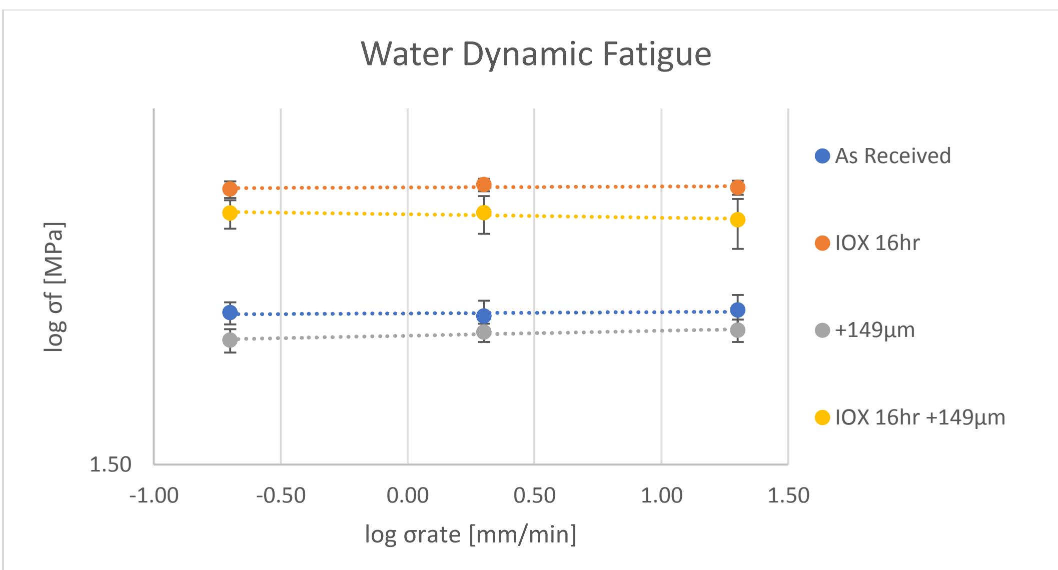

Figure 9: Dynamic fatigue plot for the water samples

Table 1: Three different m values for each rate, along with the n value for each group tested

	Air									Water			
Group	As Received	63µm	149µm	IOX 4hr	IOX 16hr	IOX 4hr +63µm	IOX 4hr +149µm	IOX 16hr +63µm	IOX 16hr +149µm	As Received	IOX 16hr	149µm	IOX 16hr +149µm
m (slow rate)	6.10	14.82	11.07	13.59	13.97	4.70	3.17	12.33	4.76	11.88	12.31	11.77	6.87
m (medium rate)	5.61	11.79	9.26	11.61	18.42	4.87	2.89	5.05	6.60	7.75	16.07	14.25	3.76
m (fast rate)	6.92	9.28	10.34	9.55	13.89	4.30	3.69	11.22	4.15	7.37	14.71	11.99	3.19
n	23.69	-37.10	23.33	33.48	-57.82	-127.58	11.85	-14.57	-77.92	191.31	211.77	52.76	-62.73

Figure 10 contains the Weibull plot for the samples which were just ABR and then ABR followed by IOX. These samples were submerged in water before breaking (submerge) and the samples which were tested under water and broke while being in the water (brake). Table 2 supplies the m values for these submerged and brake samples tested at the 2mm/min. Note, n values couldn't be obtained due to the samples being tested at only one rate.

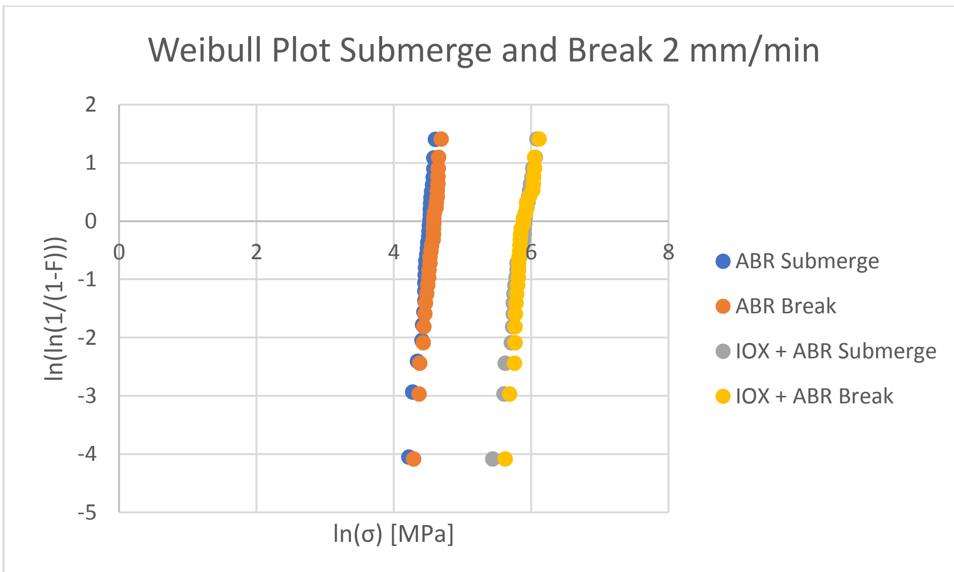

Figure 10: Break in Water Weibull Plot

Table 2: m values for addition testing of submerged and breaking in water samples

	Submerged in Water		Break in Water	
	149µm	149µm + IOX 16hr	149µm	149µm + IOX 16hr
m value	14.02	8.57	12.91	10.03

RESULTS

The glass used for this thesis is AR Glass, which is produced by Schott. AR glass is a unique type of soda -lime-silicate glass whose chemical composition is as follows 69% SiO_2 1% B_2O_3 3% K_2O 4% Al_2O_3 13% Na_2O 2% BaO 5% CaO 3% MgO. The main components are in approximate weight percent.[5]

As a glass is ion exchanged, the stress enhanced corrosion or slow crack growth constant (n) increases. The longer the ion exchange time, the larger compressive stress is added to the glass surface and the larger the n value obtained. For every order of magnitude in which the loading rate is increased, the glass will fail at a stress that is 40% larger than the previous failure stress. Figure 11 shows that the theoretical dynamic fatigue curve and Table 3 shows the theoretical n values. The n values approximately increase by a total of 3 when the compressive stress, influenced by ion exchange time, is increased by 100MPa.

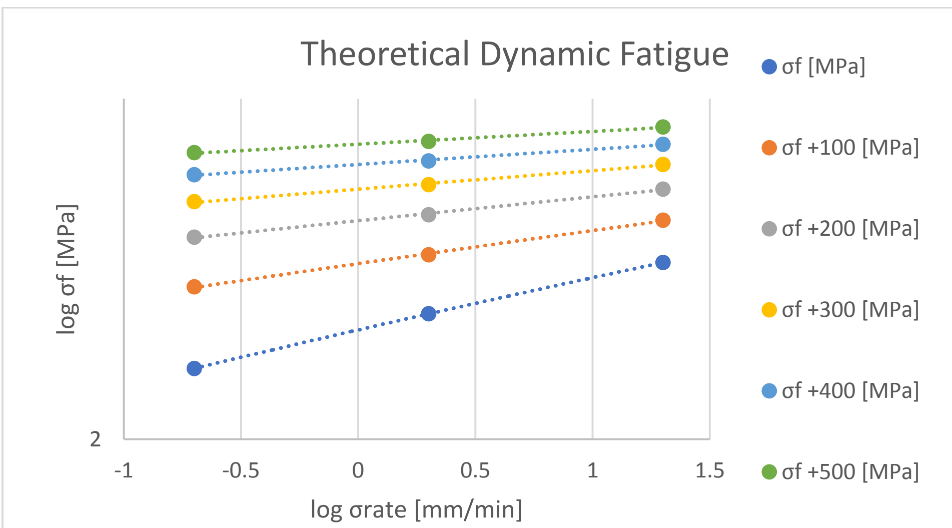

Figure 11: Theoretical Dynamic Fatigue Plot

Table 3: Theoretical n Values

	n value
σf	5.8
σf +100	9.1
σf +200	12.4
σf +300	15.6
σf +400	18.8
σf +500	22.0

Both treatments, the IOX and abrasion, impacted the strengths of the glass. The abrasion, as expected weakened the glass, and the IOX increased the glass strength. The abrasion lowered the strength of the glass, regardless of testing, by approximately 25 to 50 MPa. Meanwhile the IOX treatment increased the strength of the glass generally by about a minimum of 200 MPa. The testing rates which were used didn't impact the strength of the glass to a large extent. The faster testing rates didn't always provide larger results, and when it did provide larger strengths it was only by a few MPa.

The Weibull moduli shows if the glass is consistently breaking at the same stress or not. The larger the Weibull moduli (slope of m) the more consistent the glass strength. Between the testing rates for the glass groups which had the same alterations made to it, the Weibull moduli is inconsistent.

The characteristic strength can be determined when the y-axis is equal to zero on a Weibull modulus figure. When ln(ln(1/(1-F))) = 0 that is defined as the characteristic strength. This characteristic strength can be used to compare strength values of different Weibull moduli.

It was previously stated that for every order of magnitude in loading rate in which the glass is tested the glass should break at a stress 40% greater than the previous stress. In the failure strengths obtained, this 40% increase in strength is not observed. This brings into question the loading rate and how the strengths did not change, when ideally the faster rates should have larger strengths. When the glass is being tested at a slower loading rate there is more time for interaction between the crack tip and the water. Ideally the water should grow the crack and interact. Meanwhile if the glass is being tested at a faster rate then there is no time for an interaction between the crack tip and water. It is possible that the IOX treatment was not allowing for water to reach the crack tip, and as a result there would be no lengthening of the crack and no water assisted failure.

The n values obtained do not with the theoretical n values, which range between 5 to 20, which do not match that of the measured values. The measure n values are also very inconsistent, ranging from about 200 to about -125 depending on which samples are being observed. A negative n value would suggest that the glass is getting stronger while aged under stress. Positive n values indicate that the glass is getting weaker under stress and with an increase in time. Overall a larger positive n value means that the glass is less susceptible to slow crack growth, while a smaller positive n value shows the glass is more susceptible to slow crack growth. The IOX 4hr + 63µm, IOX 4hr, and 149µm, all of which were tested in air, had the most reasonable n values of all the tested groups. If there is no water present there will be no attack on the crack tip, even if the glass is sensitive to water. For the groups tested which have large n values, it could be possible that the water is not reaching the crack tip, due to the IOX treatment which was done to the glass, so no stress enhanced corrosion is occurring in the first place.

The observed slow crack growth constant, n, do not match that calculated from the theoretical. This shows that the theoretical data used to determine what the n value is incorrect. It is difficult to predict the n value when multiple variables are used. The theoretical data only takes into account the IOX time period, due to the corresponding compressive stress placed on the surface of the glass. The theoretical value does not consider the abrasion or introduction of flaws on the surface of the glass. The combination of both ion exchange and abrasion change the distribution of flaws present on the surface.

A possible issue in the experiment is a a possible inconsistency in the humidity in the mechanical testing room, it is a “controlled humidity”. However, the humidity reader has been found to be incorrect with providing the actual humidity. If some samples were tested in more humid days, then those samples would have possibly had more interactions between water and the crack tip.

The n value as a function of sample type and the treatment done to the samples can be found in Figure 12. This figure shows the inconsistency of the n value. The Weibull moduli for both the air and water samples as a function of loading rate can be found in Figures 13 and 14. These figures show that the modulus is inconsistent between the three different loading rates. The characteristic strength as a function of loading rate for both the air and water samples can be found in Figure 15 and 16. The characteristic strength has little change depending on the loading rate, which is not what is expected. This shows that there is no change in strength as you increase the loading rate, the faster rates are not stronger than the slower rates.

The data regarding the samples which were tested after submerging in water and then testing and breaking in water supplies some interesting information. From the data it can be determined that there is a small difference between testing after the samples were submerged in water for a few minutes before breaking and testing while the rods were immersed in water for the testing.

Recent data obtained just before the final due date for the thesis indicates a possible additional affect on measured strength, this data can be found in Table 4. The data is ball on ring testing done by a Budziszewski. The data obtained for this thesis, along with the data obtained by Budziszewski, might possibly provide an answer for the unusually high n values and negative n values. It is possible that the Instron load cell is not recording the actual breaking strength at high load rates.

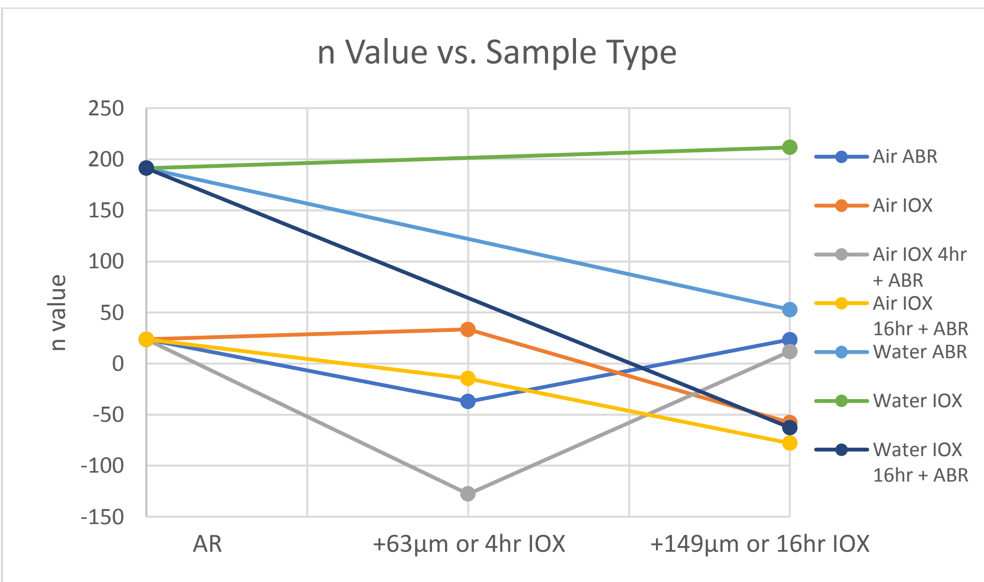

Figure 12: The n value as a function of sample

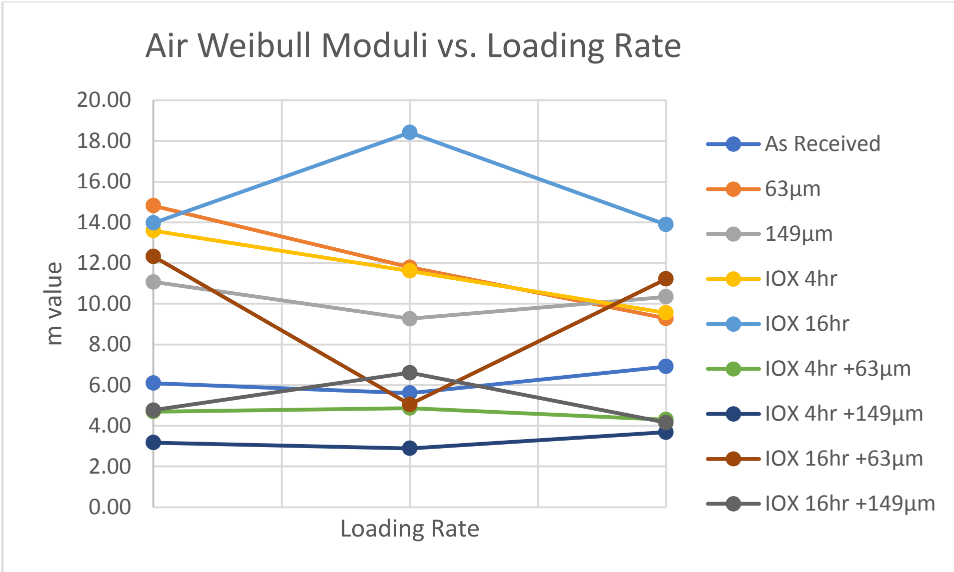

Figure 13: Weibull modulus for samples tested in air as a function of loading rate

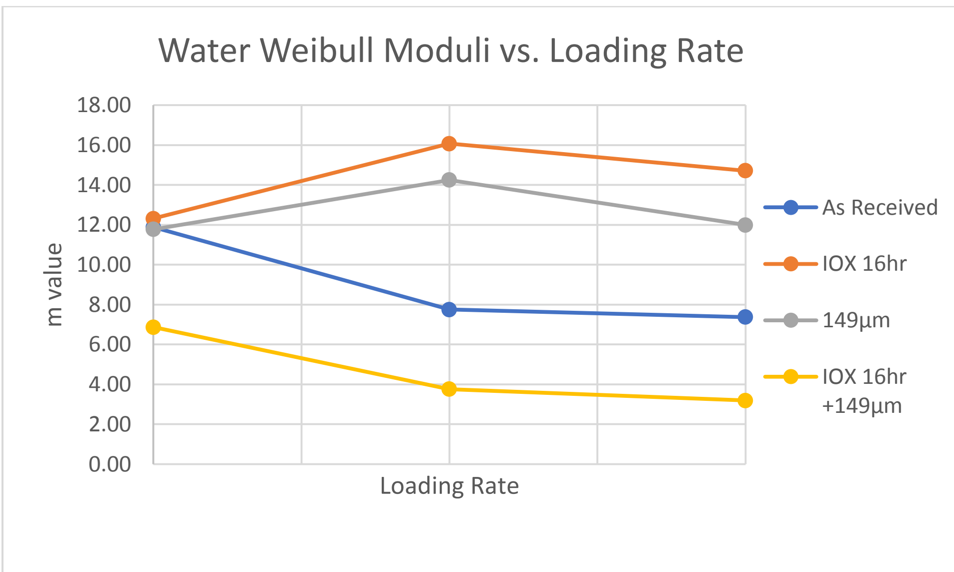

Figure 14: Weibull modulus for water samples as a function of loading rate

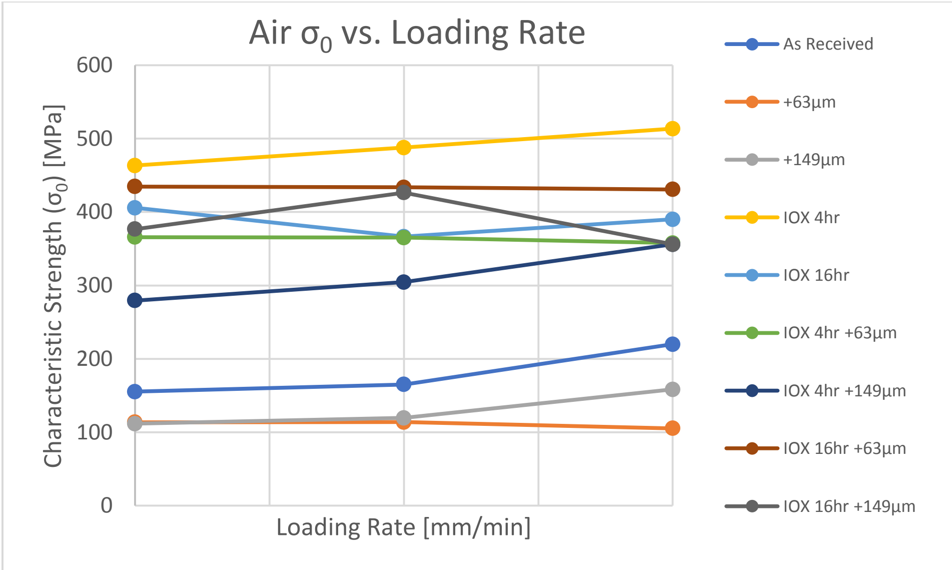

Figure 15: Air sample characteristic strength as a function of loading rate

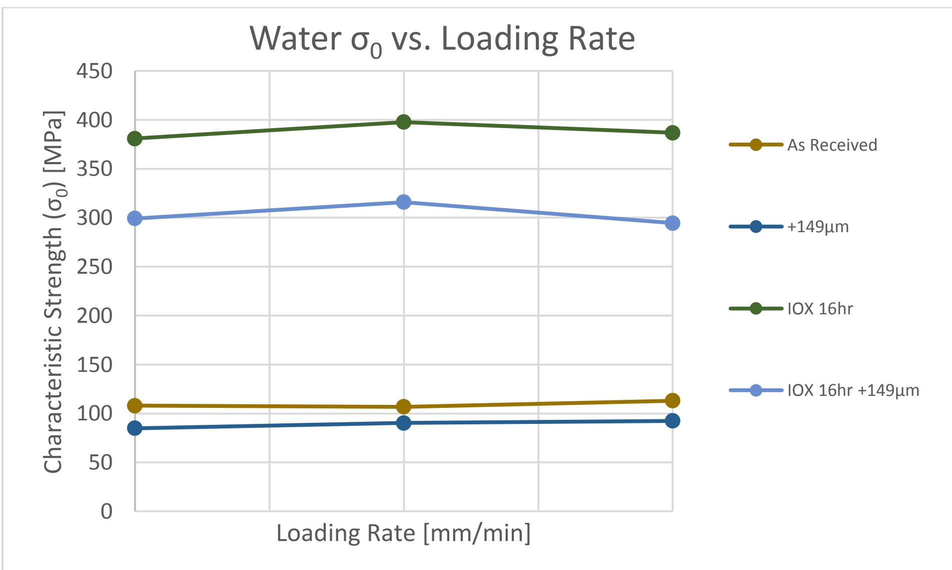

Figure 16: Water sample characteristic strength as a function of loading rate

Table 4: Ball on ring test data

mm/min	Mean MOR	St. Dev.
0.7	166.8	16.3
7	168.7	21.7
70	124.1	14.9

CONCLUSION

The surface stresses induced through chemical strengthening by ion exchange reduced the effect of stress-induced slow crack or water is restrained from interacting crack tip. The data was expected followed the expected theoretical data, in which for every order of magnitude of an increase in testing rate the glass fails at a stress that is 40% larger than the previous strength. The model which is used to calculate this data could be incorrect. The n value is difficult to predict when both IOX and abrasion is altered, in combination both the IOX and abrasion change the flaw distribution.

REFERENCE

1. J. E. Shelby, *Introduction to Glass Science and Technology,* 2nd ed. The Royal Society of Chemistry, Cambridge, UK, 2005.
2. Corning Incorporated, “The Secret of Tough Glass: Ion Exchange” (2018). Accessed on: February 2018. Available at < https://www.corning.com/worldwide/en/innovation/the-glass-age/science-of-glass/the-secret-of-tough-glass-ion-exchange.html>
3. Krishan K. Chawla, *Composite Materials Science and Engineering,* 3rd ed. Springer, New York, 2012.
4. William D. Callister and David G. Rethwisch, *Fundamentals of Materials Science and Engineering An Integrated Approach,* 4th ed. John Wiley & Sons, Inc, Hoboken, NJ, 2012.
5. Schott, “AR-Glass Tubing and Rod of Special Glass. Mitterteich, Germany, 2018.
6. V. Rosa, H. N. Yoshimura, M. M. Pinto, C. Fredericci, and P. F. Cesar, “Effect of ion exchange on strength and slow crack growth of a dental porcelain,” *Dent. Mater. J.*, **25** 736-43 (2008).

APPENDIX

Table A1: Air as Received Glass Data

None	1 mm/min		None	7 mm/min		None 20 mm/min		
	P	MOR		P	MOR		P	MOR
1	117.93	93.89331	1	128.06	101.9586	1	143.09	113.9252
2	130.57	103.957	2	129.57	103.1608	2	160.24	127.5796
3	141.61	112.7468	3	136.35	108.5589	3	166.51	132.5717
4	142.58	113.5191	4	138.78	110.4936	4	166.53	132.5876
5	158.17	125.9315	5	159.06	126.6401	5	177.72	141.4968
6	162.07	129.0366	6	163.82	130.4299	6	180.06	143.3599
7	164.06	130.621	7	165.25	131.5685	7	186.32	148.3439
8	165.04	131.4013	8	186.25	148.2882	8	189.99	151.2659
9	169.72	135.1274	9	191.69	152.6194	9	199.61	158.9252
10	174.65	139.0525	10	206.01	164.0207	10	201.05	160.0717
11	178.16	141.8471	11	207.73	165.3901	11	207.89	165.5175
12	178.55	142.1576	12	214.57	170.836	12	209.22	166.5764
13	196.84	156.7197	13	218.25	173.7659	13	217.37	173.0653
14	206.45	164.371	14	220.56	175.6051	14	221.02	175.9713
15	207.36	165.0955	15	221.67	176.4889	15	221.18	176.0987
16	207.91	165.5334	16	221.8	176.5924	16	226.5	180.3344
17	218.21	173.7341	17	226.62	180.4299	17	251.07	199.8965
18	228.27	181.7436	18	227.25	180.9315	18	255.66	203.551
19	232.05	184.7532	19	232.9	185.4299	19	256.25	204.0207
20	245.83	195.7245	20	234.04	186.3376	20	277.95	221.2978
	SUM	2886.967		SUM	3049.546		SUM	3276.457
	AVG	144.3483		AVG	152.4773		AVG	163.8229
	STD	27.52026		STD	29.06089		STD	27.90502

Table A2: Air +63µm Glass Data

AB +63 1 mm/min			AB +63 7 mm/min			AB +63 20 mm/min		
	P	MOR		P	MOR		P	MOR
1	117.79	93.78185	1	114.01	90.77229	1	101.97	81.18631
2	127.49	101.5048	2	115.78	92.18153	2	102.49	81.60032
3	127.55	101.5525	3	120.76	96.1465	3	108.04	86.01911
4	127.86	101.7994	4	120.82	96.19427	4	108.75	86.58439
5	130.08	103.5669	5	123.28	98.15287	5	109.1	86.86306
6	132.39	105.4061	6	128.42	102.2452	6	113.62	90.46178
7	132.68	105.6369	7	130.41	103.8296	7	117.26	93.35987
8	132.71	105.6608	8	134.03	106.7118	8	119.76	95.35032
9	133.4	106.2102	9	134.54	107.1178	9	119.81	95.39013
10	136.67	108.8137	10	136.64	108.7898	10	122.91	97.85828
11	137.61	109.5621	11	137.88	109.7771	11	125.66	100.0478
12	138.13	109.9761	12	139.74	111.258	12	130.03	103.5271
13	139.82	111.3217	13	140.05	111.5048	13	130.22	103.6783
14	141.26	112.4682	14	141.15	112.3806	14	132.69	105.6449
15	141.27	112.4761	15	149.57	119.0844	15	134.21	106.8551
16	142.04	113.0892	16	151.57	120.6768	16	137.82	109.7293
17	143.04	113.8854	17	153.29	122.0462	17	140.27	111.6799
18	151.77	120.836	18	155.17	123.543	18	142.81	113.7022
19	159.75	127.1895	19	155.83	124.0685	19	152.68	121.5605
20	163.74	130.3662	20	159.03	126.6162	20	160.34	127.6592
	SUM	2195.104		SUM	2183.097		SUM	1998.758
	AVG	109.7552		AVG	109.1549		AVG	99.9379
	STD	8.52999		STD	10.77778		STD	12.60263

Table A3: Air +149μm Glass Data

AB +149	1 mm/min		AB +149	7 mm/min		AB +149 20 mm/min		
	P	MOR		P	MOR		P	MOR
1	99.88	79.52229	1	106.88	85.09554	1	112.48	89.55414
2	111.82	89.02866	2	113.24	90.15924	2	121.81	96.98248
3	120.21	95.7086	3	117.27	93.36783	3	127.68	101.6561
4	120.42	95.8758	4	121.57	96.7914	4	137.06	109.1242
5	120.93	96.28185	5	130.37	103.7978	5	139.12	110.7643
6	127.79	101.7436	6	134.98	107.4682	6	145.12	115.5414
7	127.98	101.8949	7	137.83	109.7373	7	145.46	115.8121
8	128.6	102.3885	8	138.83	110.5334	8	147.66	117.5637
9	130.15	103.6226	9	141.1	112.3408	9	150.38	119.7293
10	132.98	105.8758	10	141.79	112.8901	10	151.64	120.7325
11	133.69	106.4411	11	142.39	113.3678	11	153.52	122.2293
12	137.12	109.172	12	144.07	114.7054	12	155.27	123.6226
13	139.44	111.0191	13	150.65	119.9443	13	157.14	125.1115
14	141.15	112.3806	14	152.28	121.242	14	159.91	127.3169
15	141.84	112.9299	15	154.38	122.914	15	160.29	127.6194
16	145.35	115.7245	16	158.49	126.1863	16	163.44	130.1274
17	146.79	116.871	17	160.53	127.8105	17	168.16	133.8854
18	146.9	116.9586	18	161.74	128.7739	18	172.41	137.2691
19	148.71	118.3997	19	168.7	134.3153	19	175.05	139.371
20	162.14	129.0924	20	174.33	138.7978	20	177.3	141.1624
	SUM	2120.932		SUM	2270.239		SUM	2405.175
	AVG	106.0466		AVG	113.5119		AVG	120.2588
	STD	11.15709		STD	14.23923		STD	13.43865

Table A4: Air IOX 4hr Glass Data

IOX 4hr 1 mm/min			IOX 4hr 7 mm/min			IOX 4hr 20 mm/min		
	P	MOR		P	MOR		P	MOR
1	438.2	348.8854	1	449.73	358.0653	1	476.25	379.1799
2	465.07	370.2787	2	491.67	391.457	2	497.52	396.1146
3	521.92	415.5414	3	510.92	406.7834	3	513.71	409.0048
4	540.19	430.0876	4	518.89	413.129	4	532.54	423.9968
5	541.66	431.258	5	536.77	427.3646	5	540.27	430.1513
6	558.45	444.6258	6	547.51	435.9156	6	575.19	457.9538
7	558.93	445.008	7	574.37	457.301	7	584.52	465.3822
8	559.86	445.7484	8	586.25	466.7596	8	584.82	465.621
9	560.65	446.3774	9	591	470.5414	9	590.15	469.8646
10	561.11	446.7436	10	604.92	481.6242	10	610.93	486.4092
11	562.09	447.5239	11	606.57	482.9379	11	613.23	488.2404
12	565.22	450.0159	12	617.07	491.2978	12	625.57	498.0653
13	566.26	450.8439	13	618.02	492.0541	13	629.94	501.5446
14	567.08	451.4968	14	625.01	497.6194	14	659.84	525.3503
15	586.01	466.5685	15	626.42	498.742	15	662.71	527.6354
16	587.31	467.6035	16	629.09	500.8678	16	685.02	545.3981
17	598.45	476.4729	17	630.16	501.7197	17	693.33	552.0143
18	610.7	486.2261	18	649.11	516.8073	18	720.02	573.2643
19	619.88	493.535	19	654.68	521.242	19	725.36	577.5159
20	624.26	497.0223	20	666.68	530.7962	20	732.88	583.5032
	SUM	8911.863		SUM	9343.025		SUM	9756.21
	AVG	445.5932		AVG	467.1513		AVG	487.8105
	STD	35.30938		STD	45.94646		STD	59.69124

Table A5: Air IOX 16hr Glass Data

IOX 16hr 1 mm/min			IOX 16hr 7 mm/min			IOX 16hr 20 mm/min		
	P	MOR		P	MOR		P	MOR
1	392.57	312.5557	1	405.1	322.5318	1	368.02	293.0096
2	429.49	341.9506	2	407.37	324.3392	2	414.73	330.199
3	434.37	345.836	3	409.51	326.043	3	415.59	330.8838
4	450.88	358.9809	4	418.34	333.0732	4	435.27	346.5525
5	459.85	366.1226	5	424.27	337.7946	5	455.1	362.3408
6	464.79	370.0557	6	427.29	340.199	6	455.17	362.3965
7	472.41	376.1226	7	431.46	343.5191	7	468.03	372.6354
8	485.13	386.25	8	435.54	346.7675	8	468.22	372.7866
9	488.59	389.0048	9	438.02	348.742	9	470.65	374.7213
10	497.53	396.1226	10	438.72	349.2994	10	474.75	377.9857
11	513.01	408.4475	11	443.75	353.3041	11	482.52	384.172
12	514.64	409.7452	12	446.59	355.5653	12	489.32	389.586
13	518.42	412.7548	13	454.4	361.7834	13	492.06	391.7675
14	518.8	413.0573	14	461.7	367.5955	14	494.08	393.3758
15	522.75	416.2022	15	471.07	375.0557	15	496.54	395.3344
16	526.59	419.2596	16	474.77	378.0016	16	497.31	395.9475
17	532.31	423.8137	17	483.39	384.8646	17	500.45	398.4475
18	532.82	424.2197	18	486.22	387.1178	18	511.47	407.2213
19	533.64	424.8726	19	489.23	389.5143	19	519.35	413.4952
20	535.03	425.9793	20	496.06	394.9522	20	533.61	424.8487
	SUM	7821.354		SUM	7120.064		SUM	7517.707
	AVG	391.0677		AVG	356.0032		AVG	375.8854
	STD	32.05969		STD	22.28206		STD	30.92792

Table A6: Air IOX 4hr +63μm Glass Data

IOX 4hr +63 1 mm/min			IOX 4hr +63 7 mm/min			IOX 4hr +63 20 mm/min		
	P	MOR		P	MOR		P	MOR
1	227.54	181.1624	1	227.33	180.9952	1	168.66	134.2834
2	253.17	201.5685	2	257.57	205.0717	2	249.34	198.5191
3	274.87	218.8455	3	297.22	236.6401	3	336.4	267.8344
4	277.99	221.3296	4	307.22	244.6019	4	346.62	275.9713
5	396.16	315.414	5	351.45	279.8169	5	352.68	280.7962
6	397.83	316.7436	6	360.58	287.086	6	363.17	289.1481
7	398.33	317.1417	7	377.49	300.5494	7	374.92	298.5032
8	430.46	342.7229	8	417.82	332.6592	8	375.32	298.8217
9	431.54	343.5828	9	425.33	338.6385	9	396.34	315.5573
10	444	353.5032	10	427.49	340.3583	10	422.45	336.3455
11	459.92	366.1783	11	434.36	345.828	11	434.63	346.043
12	462.16	367.9618	12	446.69	355.6449	12	454.46	361.8312
13	468.79	373.2404	13	451.54	359.5064	13	459.75	366.043
14	471.75	375.5971	14	485.65	386.664	14	461.79	367.6672
15	476.41	379.3073	15	492.99	392.508	15	462.94	368.5828
16	482.54	384.1879	16	498.04	396.5287	16	500.42	398.4236
17	486.96	387.707	17	525.51	418.3997	17	503.16	400.6051
18	494.47	393.6863	18	526.45	419.1481	18	534.89	425.8678
19	502.03	399.7054	19	545.88	434.6178	19	538.57	428.7978
20	536.86	427.4363	20	547.59	435.9793	20		0
	SUM	6667.022		SUM	6691.242		SUM	6159.642
	AVG	333.3511		AVG	334.5621		AVG	324.1917
	STD	69.94458		STD	74.18887		STD	100.4934

Table A7: Air IOX 4hr +149µm Glass Data

IOX 4hr +149 1 mm/min			IOX 4hr +149 7 mm/min			IOX 4hr +149 20 mm/min		
	P	MOR		P	MOR		P	MOR
1	119.37	95.03981	1	109.91	87.50796	1	183.84	146.3694
2	177.5	141.3217	2	133.09	105.9634	2	216.18	172.1178
3	188.26	149.8885	3	191.48	152.4522	3	239.37	190.5812
4	193.62	154.1561	4	219.67	174.8965	4	263.46	209.7611
5	203.92	162.3567	5	257.5	205.0159	5	279.63	222.6354
6	239.65	190.8041	6	267.37	212.8742	6	326.82	260.207
7	276.42	220.0796	7	303.36	241.5287	7	368.64	293.5032
8	287.69	229.0525	8	307.9	245.1433	8	401.23	319.4506
9	292.96	233.2484	9	320.78	255.3981	9	410.41	326.7596
10	298.27	237.4761	10	328.28	261.3694	10	427.13	340.0717
11	336.07	267.5717	11	335.32	266.9745	11	449.36	357.7707
12	343.19	273.2404	12	384.92	306.465	12	452.02	359.8885
13	387.19	308.2723	13	385.22	306.7038	13	454.33	361.7277
14	401.12	319.3631	14	414.49	330.008	14	465.1	370.3025
15	401.72	319.8408	15	432.67	344.4825	15	473.43	376.9347
16	421.95	335.9475	16	450.13	358.3838	16	475.76	378.7898
17	460	366.242	17	457.26	364.0605	17	487.78	388.3599
18	464.34	369.6975	18	471.61	375.4857	18	506.03	402.8901
19	464.9	370.1433	19	494.13	393.4156	19	581.63	463.0812
20		0	20	512.72	408.2166	20	584.87	465.6608
	SUM	4743.742		SUM	5396.346		SUM	6406.863
	AVG	249.6706		AVG	269.8173		AVG	320.3432
	STD	97.67297		STD	91.16782		STD	90.09507

Table A8: Air IOX 16hr +63µm Glass Data

IOX 16hr +63 1 mm/min			IOX 16hr +63 7mm/min			IOX 16hr +63 20 mm/min		
	P	MOR		P	MOR		P	MOR
1	406.5	323.6465	1	248.73	198.0334	1	325.17	258.8933
2	453.91	361.3933	2	299.72	238.6306	2	346.02	275.4936
3	455.82	362.914	3	359.68	286.3694	3	348.88	277.7707
4	479.49	381.7596	4	463.62	369.1242	4	355.51	283.0494
5	488.33	388.7978	5	468.42	372.9459	5	372.12	296.2739
6	491.46	391.2898	6	498.04	396.5287	6	392.93	312.8424
7	495.83	394.7691	7	500.1	398.1688	7	407.62	324.5382
8	520.44	414.3631	8	510.27	406.2659	8	407.8	324.6815
9	520.9	414.7293	9	522.42	415.9395	9	408.52	325.2548
10	527.64	420.0955	10	529.43	421.5207	10	412.88	328.7261
11	529.73	421.7596	11	530.93	422.715	11	418.66	333.328
12	542.84	432.1975	12	532.1	423.6465	12	432.39	344.2596
13	554.03	441.1067	13	540.72	430.5096	13	434.18	345.6847
14	555.33	442.1417	14	546.25	434.9124	14	438.36	349.0127
15	559.79	445.6927	15	546.37	435.008	15	440.52	350.7325
16	568.03	452.2532	16	563.91	448.9729	16	443.84	353.3758
17	569.53	453.4475	17	566.19	450.7882	17	447.31	356.1385
18	581.53	463.0016	18	567.36	451.7197	18	465.72	370.7962
19	583.76	464.7771	19	578.52	460.6051	19	470.76	374.8089
20	600.88	478.4076	20	582.37	463.6704	20	471.46	375.3662
	SUM	8348.543		SUM	7926.075		SUM	6561.027
	AVG	417.4271		AVG	396.3037		AVG	328.0514
	STD	39.35341		STD	71.32895		STD	33.62229

Table A9: Air IOX 16hr +149μm Glass Data

IOX 16hr +149 1 mm/min			IOX 16hr +149 7 mm/min			IOX 16hr +149 20 mm/min		
	P	MOR		P	MOR		P	MOR
1	207.92	165.5414	1	287.94	229.2516	1	153.21	121.9825
2	291	231.6879	2	348.19	277.2213	2	252.48	201.0191
3	317.78	253.0096	3	399.86	318.3599	3	337.32	268.5669
4	325.75	259.3551	4	435.93	347.078	4	374.9	298.4873
5	329.26	262.1497	5	463.63	369.1322	5	404.88	322.3567
6	359.52	286.242	6	469.26	373.6146	6	407.12	324.1401
7	438.3	348.965	7	509.21	405.422	7	412.11	328.1131
8	441.37	351.4092	8	514.05	409.2755	8	418.87	333.4952
9	449.6	357.9618	9	515.25	410.2309	9	420.32	334.6497
10	453.52	361.0828	10	515.35	410.3105	10	421.82	335.8439
11	471.31	375.2468	11	525.76	418.5987	11	423.18	336.9268
12	471.85	375.6768	12	525.9	418.7102	12	423.62	337.2771
13	475.48	378.5669	13	530.67	422.508	13	428.03	340.7882
14	479.75	381.9666	14	540.07	429.992	14	429.46	341.9268
15	490.23	390.3105	15	541.18	430.8758	15	433.41	345.0717
16	491.94	391.672	16	547.78	436.1306	16	441.63	351.6162
17	510.17	406.1863	17	555.1	441.9586	17	442.98	352.6911
18	533.88	425.0637	18	578.21	460.3583	18	455.06	362.3089
19	551.95	439.4506	19	578.97	460.9634	19	458.42	364.9841
20	555.92	442.6115	20	592.7	471.8949	20	472.64	376.3057
	SUM	6884.156		SUM	7941.887		SUM	6378.551
	AVG	344.2078		AVG	397.0943		AVG	318.9275
	STD	73.76086		STD	60.89004		STD	58.46692

Table A10: Water As Received Glass Data

Nothing	0.2 mm/min		Nothing	2 mm/min		Nothing	20 mm/min	
	P	MOR		P	MOR		P	MOR
1	104.80	83.44	1.00	90.67	72.19	1.00	105.01	83.61
2	108.92	86.72	2.00	95.20	75.80	2.00	105.84	84.27
3	115.01	91.57	3.00	105.00	83.60	3.00	107.72	85.76
4	118.84	94.62	4.00	108.34	86.26	4.00	108.73	86.57
5	119.26	94.95	5.00	109.79	87.41	5.00	111.28	88.60
6	122.61	97.62	6.00	112.43	89.51	6.00	112.78	89.79
7	123.33	98.19	7.00	115.45	91.92	7.00	115.77	92.17
8	128.71	102.48	8.00	119.28	94.97	8.00	127.97	101.89
9	129.78	103.33	9.00	121.84	97.01	9.00	130.25	103.70
10	130.51	103.91	10.00	126.96	101.08	10.00	132.73	105.68
11	134.70	107.25	11.00	129.37	103.00	11.00	132.99	105.88
12	135.05	107.52	12.00	131.78	104.92	12.00	135.29	107.71
13	135.09	107.56	13.00	134.60	107.17	13.00	143.31	114.10
14	135.30	107.72	14.00	136.33	108.54	14.00	144.91	115.37
15	135.52	107.90	15.00	136.87	108.97	15.00	145.33	115.71
16	136.52	108.69	16.00	137.94	109.82	16.00	153.26	122.02
17	137.90	109.79	17.00	141.70	112.82	17.00	156.79	124.83
18	143.41	114.18	18.00	155.86	124.09	18.00	159.41	126.92
19	144.09	114.72	19.00	157.02	125.02	19.00	167.02	132.98
20	162.31	129.23	20.00	158.70	126.35	20.00	167.80	133.60
	SUM	2071.39		SUM	2010.45		SUM	2121.17
	AVG	103.57		AVG	100.52		AVG	106.06
	STD	10.23		STD	15.13		STD	16.32

Table A11: Water +149µm Glass Data

149+	0.2 mm/min		149+	2 mm/min		149+	20 mm/min	
	P	MOR		P	MOR		P	MOR
1	80.65	64.21178	1	86.26	68.67834	1	86.67	69.00478
2	85.08	67.73885	2	94.68	75.38217	2	94.75	75.4379
3	91.89	73.16083	3	99.98	79.60191	3	96.94	77.18153
4	92.25	73.44745	4	100.82	80.2707	4	99.19	78.97293
5	95.67	76.17038	5	102.17	81.34554	5	102.2	81.36943
6	96.41	76.75955	6	102.33	81.47293	6	107.94	85.93949
7	98.1	78.1051	7	108.43	86.32962	7	108.07	86.04299
8	98.43	78.36783	8	110.53	88.00159	8	110.74	88.16879
9	98.77	78.63854	9	111.36	88.66242	9	111.76	88.98089
10	103.01	82.01433	10	111.71	88.94108	10	112.02	89.1879
11	103.04	82.03822	11	112.87	89.86465	11	112.47	89.54618
12	103.09	82.07803	12	113.49	90.35828	12	113.4	90.28662
13	105.99	84.38694	13	114.15	90.88376	13	114.35	91.04299
14	106.29	84.6258	14	114.57	91.21815	14	118.14	94.06051
15	110.42	87.91401	15	114.86	91.44904	15	119.38	95.04777
16	111.22	88.55096	16	115.32	91.81529	16	119.43	95.08758
17	113.73	90.54936	17	116.79	92.98567	17	122.48	97.51592
18	113.87	90.66083	18	116.93	93.09713	18	124.45	99.08439
19	116.78	92.97771	19	119.98	95.52548	19	126.59	100.7882
20	120.69	96.09076	20	120.12	95.63694	20	127.83	101.7755
	SUM	1628.487		SUM	1741.521		SUM	1774.522
	AVG	81.42436		AVG	87.07604		AVG	88.72611
	STD	8.133916		STD	6.91624		STD	8.60605

Table A12: Water IOX 16hr Glass Data

IOX 16hr	0.2 mm/min		IOX 16hr	2 mm/min		IOX 16hr	20 mm/min	
	P	MOR		P	MOR		P	MOR
1	370.7	295.1433	1	434.07	345.5971	1	407.51	324.4506
2	381.07	303.3997	2	440.1	350.3981	2	418.4	333.121
3	400.68	319.0127	3	442.46	352.2771	3	422.45	336.3455
4	415.45	330.7723	4	444.68	354.0446	4	429.61	342.0462
5	421.98	335.9713	5	448.67	357.2213	5	433.32	345
6	426.2	339.3312	6	451.15	359.1959	6	440.27	350.5334
7	443.2	352.8662	7	457.82	364.5064	7	450.98	359.0605
8	453.1	360.7484	8	463.67	369.164	8	458.24	364.8408
9	462.48	368.2166	9	475.88	378.8854	9	459.25	365.6449
10	466.08	371.0828	10	477.73	380.3583	10	459.42	365.7803
11	467.01	371.8232	11	485.9	386.8631	11	465.18	370.3662
12	468.1	372.6911	12	486.22	387.1178	12	469.98	374.1879
13	478.08	380.6369	13	498.84	397.1656	13	490.87	390.8201
14	488.61	389.0207	14	502.78	400.3025	14	492.48	392.1019
15	490.13	390.2309	15	510.07	406.1067	15	494.38	393.6146
16	491.24	391.1146	16	515.86	410.7166	16	503.24	400.6688
17	506.5	403.2643	17	524.08	417.2611	17	504.7	401.8312
18	509.28	405.4777	18	529.27	421.3933	18	505.03	402.0939
19	513.01	408.4475	19	538.55	428.7818	19	535.31	426.2022
20	527.24	419.7771	20	543.31	432.5717	20	539.97	429.9124
	SUM	7309.029		SUM	7699.928		SUM	7468.623
	AVG	365.4514		AVG	384.9964		AVG	373.4311
	STD	34.5743		STD	27.37539		STD	29.60549

Table A13: Water IOX 16hr +149µm Glass Data

IOX 16hr +149	0.2 mm/min		IOX 16hr +149	2 mm/min		IOX 16hr +149	20 mm/min	
	P	MOR		P	MOR		P	MOR
1	218.21	173.7341	1	116.11	92.44427	1	122.39	97.44427
2	239.84	190.9554	2	238.36	189.7771	2	145.02	115.4618
3	272.11	216.6481	3	287.09	228.5748	3	163.77	130.3901
4	317.97	253.1608	4	289.84	230.7643	4	264.85	210.8678
5	329.18	262.086	5	312.06	248.4554	5	278.62	221.8312
6	333.13	265.2309	6	344.05	273.9252	6	298.32	237.5159
7	340.9	271.4172	7	354.64	282.3567	7	342.44	272.6433
8	352.54	280.6847	8	364.2	289.9682	8	349.82	278.5191
9	358.69	285.5812	9	373.75	297.5717	9	361.65	287.9379
10	361.5	287.8185	10	380.05	302.5876	10	363.71	289.578
11	366.88	292.1019	11	382.44	304.4904	11	365.55	291.043
12	371.19	295.5334	12	384.81	306.3774	12	372.37	296.4729
13	371.76	295.9873	13	394.69	314.2436	13	377.68	300.7006
14	372.6	296.6561	14	398.28	317.1019	14	377.76	300.7643
15	373.49	297.3646	15	403.24	321.051	15	379.96	302.5159
16	379.08	301.8153	16	403.93	321.6003	16	384.24	305.9236
17	402.22	320.2389	17	404.02	321.672	17	384.33	305.9952
18	409.73	326.2182	18	404.13	321.7596	18	385.13	306.6322
19	420.61	334.8806	19	404.19	321.8073	19	387.12	308.2166
20	429.18	341.7038	20	413.63	329.3232	20	412.3	328.2643
	SUM	5589.817		SUM	5615.852		SUM	5188.718
	AVG	279.4908		AVG	280.7926		AVG	259.4359
	STD	42.96986		STD	57.11867		STD	67.61891